International Journal of Engineering Research & Technology (IJERT)
ISSN: 2278-0181
Vol. 4 Issue 07, July-2015

Molding and Testing of Frost Growth on Law Temperature Display Case Evaporator

Ass. Prof. Dr. Zainab H. Naji,
Mechanical Engineering Department
University of Technology,
Baghdad-Iraq.

Khalid Ibrahim
Mechanical Engineering Department
University of Technology
Baghdad- Iraq.

Abstract - **In this paper, the performance of the flat fin-round tube evaporator at low temperature, which is typical used in supermarket display case, has been investigated numerically and experimentally. Heat and mass transfer characteristics of the evaporator during frost formation process have been studied, and measurements have been recorded for this purpose. Empirical correlations of heat and mass transfer have been used in the present model to calculate the coefficients for air side, for refrigerant side considering that the evaporator consists of two regions (two-phase and superheated), the frost thickness and the frost accumulation on the evaporator surface. The results show that the frost thickness and the frost accumulation are increased by 5.7% and 30%, respectively, when the operating conditions, i.e. the store temperature and relative humidity, change from (T_{stor}=29.7ºC, RH_{stor}=30%) to (T_{stor}=27.6ºC, RH_{stor}=25%), and by 13.3% and 85.2%, when the conditions change to (T_{stor}=26.3ºC, RH_{stor}=20%). It is found that every 5% rise in the store relative humidity results in around 1.5 Pa air pressure drop and 70W heat exchange reduction in the evaporator, at the end of 6 hours test for typical operating conditions . New correlations have been established in the two-phase region of the evaporator for the heat transfer coefficient and the length of saturated-evaporator, with the refrigerant quality. The comparison between numerical predictions and experimental data for the frost layer growth in a humid air stream shows a satisfactory consistency regarding trends of analyzed variables. The results obtained point to the fact that the developed numerical procedure could be efficiently used to calculate the exchange heat flux of a heat exchanger during the frost layer formation**.

Key words: Frost formation, evaporator, heat and mass transfer, display case.

i. INTRODUCTION

When a heat exchanger, acting as an evaporator of a refrigerant, operates in moist air and when the fin surface has been cooled below freezing temperature of the water, a frost layer formation occurs. The frost layer represents significant thermal resistance. A reduced in the heat transfer performance of evaporator occurs due to augmented thermal resistance of the frost formation. This cause in a decrease in air-flow rate and increase pressure drop across the evaporator surface, then the evaporator began to be blockage. Large amount of work has been done on understanding the evaporator performance under frosting condition. Deniz et.al[1] investigated frost formation on fin-and -tube heat exchangers numerically. Unsteady heat and mass transfer coefficient of the air side heat transfer coefficient of the refrigerant side, air-frost layer interface temperature, the surface efficiency of the heat exchanger and the mass flow rate of the frost accumulated on the heat exchanger surface are calculated. Datta et al.[2] carried out the experiment on a vertical high temperature display cabinet under controlled laboratory conditions and analyses the observed results to identify parameters which best represent the degradation of the system performance due to frosting. Tso et.al[3] studied the dynamic behavior of an evaporator, the equations are derived in non-steady-state manner for the refrigerant and a quasi-steady

Nomenclatures

A_F	Surface area of the fin[m^2]
Ai	Surface area inner of evaporator[m^2]
A_T	Total heat transfer area on the air-side[m^2]
$A_{min,fr}$	Minimum flow area of frosted evaporator[m^2]
$A_{T,fr}$	Total heat transfer area of frosted evaporator[m^2]
Cp	Specific heat[kJ/kg.K]
D	Total evaporator depth [m]
di	Tube inside diameter of evaporator[m]
do	Tube outside diameter of evaporator[m]
f	Friction factor
F_S	Fin spacing [m]
G_{max}	Maximum mass flux[kg/s.m^2]
h	Enthalpy[kJ/kg]
h_a	Air side heat transfer coefficient[W/m^2.K]
h_r	Refrigerant side heat transfer coefficient[W/m^2.K]
h_{sg}	Enthalpy of sublimation of water vapor[kJ/kg]
h_{lat}	Latent air side heat transfer coefficient[W/m^2.K]
h_o	Total heat transfer coefficient of frost layer[W/m^2.K]
k	Thermal conductivity [W/m.K]
L	Total tube length for the evaporator[m]
$\dot{m}$	Mass flow rate[kg/s]
m_{fr}	Frost deposition rate[kg]
P_a	Air pressure drop across coil [Pa]
Q	Heat transfer rate [W]
T	Temperature [C]
t	Time[s]
W	Total evaporator width[m]
UA	The overall heat transfer coefficient of evaporator[W/m^2.K]
X_{tt}	Martinelli parameter
x	quality

Greek Symbols

ε	Fin area ratio
δ_F	Fin thickness [m]
δ_{fr}	Frost thickness [mm]
η_f	Fin efficiency
η_s	Surface efficiency
ω	Humidity ratio [kg moisture/kg dry air]
ρ	Density[kg/m^3]
μ	Viscosity [kg/s.m]
α	Void fraction
σ	Surface tension [N/m]

Subscripts

a	Air
in	Inlet
ave	Average
out	Outlet
e	Evaporator
fr	Frost
sp	Superheated
tp	Two-phase

state model with permeation for the frost. Getu et al.[4] presented an experimental analysis of evaporators in the supermarket display cabinets at low temperatures. Extensive experiments were conducted to measure store and display cabinet relative humidity, temperatures, and mass flow rates of the refrigerant. A.L. Bendaoud et.al[5] proposed a new modeling approach, accounting for heat and mass transfer as well as the hydrodynamics of the problem of the frost accumulation due to moist air flowing on a refrigeration coil cold surface which impacts negatively on performance. Christian J. L. Hermes et.al [6] predicted the time evolution of the porosity of a frost layer over a flat surface was proposed. The theoretical model was used together with experimental data obtained elsewhere to put forward a semi-empirical correlation for the frost. Bruno N. Borges et.al [7] described a quasi-

steady-state simulation model for predicting the transient behavior of a household refrigerator subjected to periodic door opening. A semi-empirical steady state sub-model was developed for the refrigeration loop, and a transient sub-model was devised to predict the energy and mass transfer into and within the refrigerated compartments as well as the evaporator frosting.

Although frost is a constant problem for low temperature applications, no complete model has been developed to predict it accurately yet. There are too many variables influencing the growth of frost. Therefore, in the present study there is a need for the development of numerical models to evaluate the performance of supermarket heat exchanger of frozen food cabinets in particular under frosted conditions and validate with experiments. To the knowledge of the researcher, most literatures mentioned above did not include the fact that the refrigerant passes through two regions (superheated/two-phase) in the evaporator.

Table (1) Test evaporator specifications.

Geometrical parameter	Characteristics
Fin material	Aluminum plate
Tube material	Aluminum
Fin thickness	0.2 [mm]
Tube I.D	6.35 [mm]
Tube O.D	7.94 [mm]
Coil length	27 [cm]
Coil width	48 [cm]
Coil depth	7 [cm]
No. of rows deep	2
No. of rows high	8
Traverse tube spacing.ST.	3.5 [cm]
Longitudinal tube spacing.SL.	3.5 [cm]
Fin type	flat

ii. EXPERIMENTAL APPROACH

Experimental investigation was carried out is vertical glass door display cabinets type (GonGord) ,which constructed from insulated walls from the inside materiality C-pentane of dimensions(198×61×48) cm length, width and depth respectively. The evaporator presented in this research is direct expansion flat fin-round tube heat exchanger and, in-line arrangement which uses R404A refrigerant. The evaporator specifications are shown in table (1).

Sensors type (hygrothermograph, STH-2) were using to measure the temperature and relative humidity of air Features indoor and outdoor, the sensors temperature range (-30C~ +50C); while the humidity range (20% ~ 99% RH). The measurement of the refrigerant temperature was taking in four points. Two of them at the inlet and outlet from the evaporator, while the third one at the compressor exit and the fourth one at the condenser exit using sensors type (Digital thermometer, ST-1A) which having temperature range (-50 C° + 80C°).See figure (1).

1	Store temperature- humidity sensor	4	Refrigerant Temperature sensor interring the evaporator
2	Discharge air temperature- humidity sensor display cabinet	5	air interring the evaporator temperature- humidity sensor
3	air leaving the evaporator temperature- humidity sensor		

Fig. (1) External Screen digital sensor on display cabinet

The operating (oily gauge) type Replacement gauge was using to measure the pressure of the refrigerant. Three oily The mass flow rate of the refrigerant can be vialed from measuring electric power consumption of the compressor using the following simple relationship [8].

$$P - E = \left(h_{r,out} - h_{r,in}\right) \times \dot{m}_r \qquad (1)$$

Where is, P: electric power (W) and E: The heat loss expressed as a percentage of P is between 5 and 7% for most compressor type. The ratio adopted in this study is (5%).

iii. OPERATING UNDER FROSTING CONDITION

The test facility must simulate realistic operating conditions for low temperature applications. For this reason, measurements were taken for small capacity low temperature refrigeration systems such as a closed door display cabinet. The recording data results of temperatures, relative humidity, pressures and refrigerant mass flow rates were taken over 10 days period at interval of 1 hour after putting

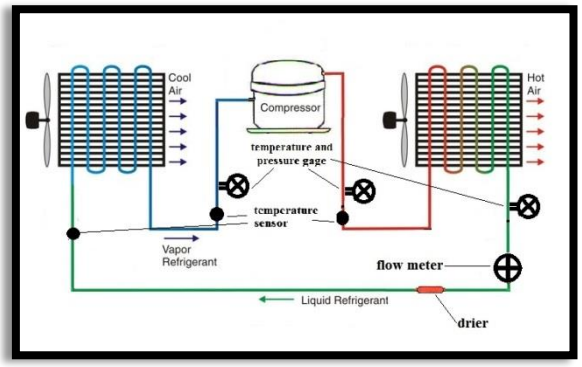

Fig. (2) Schematic diagram Measuring devices.

gauges were using in this work: the first one for low presser (250 psi) and the two others for high pressure (500psi). Turbine flow meter of type KF500 series was used to measure mass flow rate of the refrigerant. The flow meter specifications are as follows: nominal diameter is 4mm and the flow rate is (0.04~0.25) m/h the intrinsic error is 1% of reading. See figure (2)

amount of meat product (chicken,45kg) inside display cabinets.. The experimental results of frost thickness for typical case are shown in figure (3). The measurement of frost thickness was done by using high accuracy digital camera.

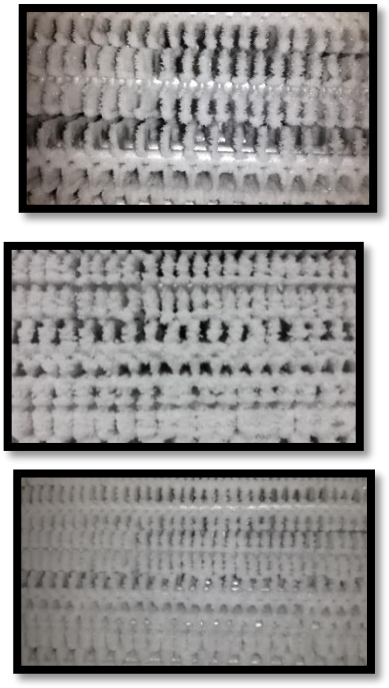

Fig. (3) Frost formation at (T_{stor}=28.7ºC,RH_{stor}=25.6%,$T_{a,in}$=−14.41ºC,$T_{r,in}$=−36ºC) after 1 hr,3hr,6hr test, respectively.

iv. MATHEMATICL MODEL

This study presents a mathematical model for predicting the frosting behavior of a fin-tube heat exchanger and evaluates the thermal performance of the heat exchanger under frosting conditions. The basic dimensions of evaporator are shown in Figures (4) and (5). While the fin density, number of tubes and mass flow rates are chosen as parameters of the study, other characteristics such as fin geometry, and tube spacing and alignment remained same throughout the studies. The evaporator model was written in a software package called Engineering Equation Solver (EES)[9]. The evaporator in the display cases has two regions; superheated and two-phase region based on the refrigerant phase. The fraction of the evaporator area is then calculated in proportion to the amount of heat transfer in each region.

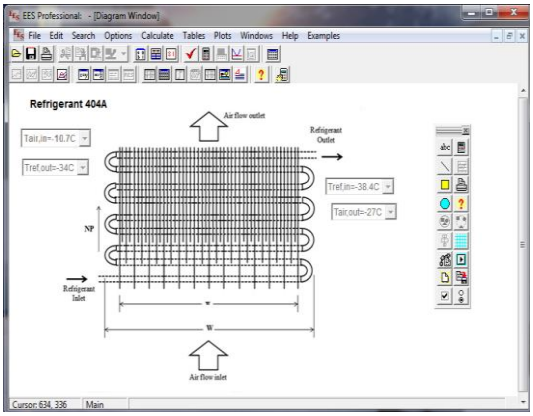

Fig. (4) Diagram Window of flat fin-round tube evaporator.

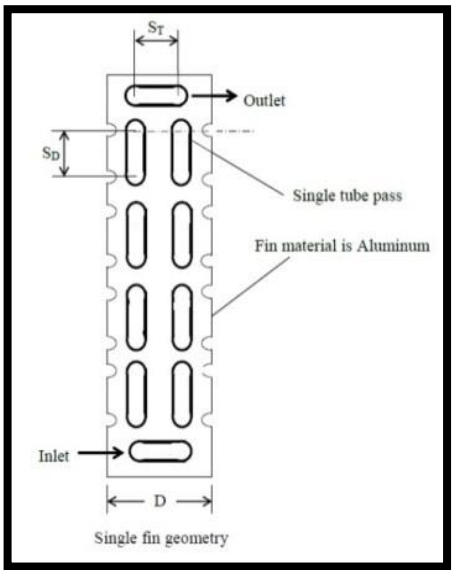

Fig. (5) Cross-sectional side view of evaporator.

A. General Assumptions

The following assumptions were used in the calculation procedure of the mathematical model to predict the performance of flat-finned-tube heat exchanger (display cabinet evaporator) applied in the low-temperature refrigeration systems.

1. Steady state operation.
2. Constant air-side convective heat transfer coefficient over entire heat exchanger.
3. Refrigerant pressure drops in the heat exchangers are negligible.
4. Mass flux of air, G_{max} , is also constant along the coil length.
5. State of the refrigerant in one element is saturated or superheated.
6. Frosting process in the evaporators is quasi-steady, where parameter calculated at time (t) is used for calculations at time (t+Δt).
7. All heat and mass transfer processes are regarded as one dimensional.
8. The air at the inlet of evaporator is perfectly mixed.

B. Heat Transfer Equations for Evaporator

The heat transfer due to the air and refrigerant in an infinitesimal control volume should be balanced. This balance can be expressed as follows:

$$Q_T = Q_{air,side} = Q_{ref,side} = Q_{tp} + Q_{SP} \quad (2)$$

Where the air-side rate of heat transfer is determined by

$$Q_{a,side} = \dot{m}_a(h_{a,in} - h_{a,out}) \quad (3)$$

The refrigerant-side rate of heat transfer is calculated from.

$$Q_{r,side} = \dot{m}_r(h_{r,out} - h_{r,in}) \quad (4)$$

Also, the rate of heat transfer over the evaporator is the sum of the heat transferred in each-element;

$$Q_T = UA_T(T_{air,ave} - T_{ref,ave}) = Q_{tp} + Q_{SP} \quad (5)$$

The heat transfer rate in the superheated region is given by:

$$Q_{SP} = h_{r,sp}A_{sp}(T_{air,in} - T_{ref,out}) \quad (6)$$

And, the heat transfer value in two-phase region is given by:

$$Q_{tp} = h_{r,tp}A_{tp}(T_{air,out} - T_{ref,in}) \quad (7)$$

Where the area fractions for each zone (superheated, two-phase) of the evaporator can be estimated:

$$A_{sp} = A_T\left(\frac{Q_{SP}}{Q_T}\right) \text{ for single-phase} \quad (8)$$

$$A_{tp} = A_T\left(\frac{Q_{tp}}{Q_T}\right) \text{ for two-phase} \quad (9)$$

Therefore the length of the evaporator tube for each region (single, two phase) can be estimated using equation the fowling equation:

$$A_{sp\ or\ tp} = NT.(\pi\ d_i L) \quad (10)$$

C. Refrigerant - Side Heat Transfer Coefficient

1. Single –Phase Region

For single-phase, the refrigerant heat transfer coefficient (h_r) is calculated using the correlation proposed by Incropera and Dewitt [10] is defined as:

$$\frac{h_r.d_i}{k} = 0.023Re^{0.8}\ pr^{0.4} \quad (11)$$

2. Tow-Phase Region

The formula of heat transfer correlation for two-phase flow was modified by Hwang et al.[11] have been used to calculate (h). This is based on the superposition principle which consists of assuming that (h).is the sum of nucleate boiling coefficient (h) and convection heat transfer coefficient (h_r) as:

$$h_r = h_{nb} + h_{bc} \quad (12)$$

Where $h_{nb}$is given by;

$$h_{nb} = \Omega(T_w - T_{sat})^{0.4}.(p_{sat} - p_l)^{0.75}.S \quad (13)$$

And h_{bc} equation is ;

$$h_{bc} = h_l.Pr^{0.6}.F.(1-x)^{0.8} \quad (14)$$

h_l is the convective heat transfer coefficient for the liquid phase calculated by Dittus-Boelter correlation (Incropera et al.)[12]. The expressions of Ω,S and F Parameters in equations(13) and (14) are given in Appendix[A].

D. Air Side Convective Heat Transfer Coefficient

$$h_a = 0.113\ Re^{0.755} pr^{1/3}\ \varepsilon^{-0.420}\frac{k_a}{do} \quad (15)$$

$300 < Re_a < 1000$, and $3.43 < \varepsilon < 5.92$

If factor becomes smaller than 3.43 the following relation be used

$$h_a = 0.113\ Re_a^{0.719}\ pr^{1/3}\ \varepsilon^{-0.407}\frac{k_a}{do} \quad (16)$$

$300 < Re_a < 1000$, $1 < \varepsilon < 5.92$

The surface efficiency (η_s)combines the fin and tube surfaces as if they are only one surface at an average surface temperature.

$$\eta_s = 1 - \frac{A_F}{A_T}(1-\eta_F) \quad (17)$$

Where (η_F) is dry fin efficiency of evaporator.

$$\eta_F = -3.429m_k^4 + 6.457m_k^3 - 4.308m_k^2 + 0.736m_k + 0.949 \quad (18)$$

Where $m_k$is fin parameter given by Karatas [13]

$$m_k = \sqrt{\frac{2h_a d_o^2}{k_F \delta_F}} \quad (19)$$

The effective heat transfer coefficient of frost (h_{eff}) can be calculated as:

$$h_{eff} = h_a + h_{lat} \quad (20)$$

The latent heat transfer coefficient (h_{lat}) is obtained from the following

$$h_{lat} = \frac{h_a h_{sg}(\omega_{in} - \omega_{out})}{Le.Cp(T_{a,in} - T_{a,out})} \quad (21)$$

Where the Lewis number (Le) is assumed to be 1. The sublimation latent heat is calculated from the correlation reported by Ismail and Salinas [14].

$$h_{sg} = 2322\left(-0.04667\left(1.8T_{r,ave} + 32\right) + 1220.1\right) \quad (22)$$

A change because of frost will be made in fin parameter (m_F) by replacing (h_a) with (h_o).

$$m_{k,fr} = \sqrt{\frac{2h_o d_o^2}{k_F \delta_F}} \quad (23)$$

Here (h_o) is total heat transfer coefficient on the frosted surface that is defined by including the frost layer thermal resistance.

$$h_o = \left(\frac{1}{h_{eff}} + \frac{\delta_{fr}}{k_{fr}}\right)^{-1} \quad (24)$$

Then, the overall heat transfer coefficient with the presence of a frost layer (including the heat and mass transfer coefficients) can be written

$$\frac{1}{(UA)_{fr}} = \frac{1}{h_r A_i} + \frac{1}{h_{eff}\eta_s A_{T,fr}} + \frac{\delta_{fr}}{k_{fr}\eta_s A_{T,fr}} \quad (25)$$

E. Air Side Pressure-Drop

The pressure drop over the evaporator is estimated using correlation suggested by kays and London (1992).

$$\Delta P = \frac{G_{max}^2}{2\rho_i}\left[(1+\sigma^2)\left(\frac{\rho_i}{\rho_i} - 1\right) + f\frac{A_{T,fr}}{A_{min,fr}}\frac{\rho_i}{\rho m}\right] \quad (26)$$

$$\sigma = \frac{A_{min,fr}}{W.D} \quad (27)$$

An important parameter in this equation arises as friction factor (f) this value is experimentally defined for dry evaporators by Karatas as [13];

$$f = 0.152Re^{-0.164}\varepsilon^{-0.331} \quad (28)$$

F. Frost Accumulation and Thickness Calculation

The frost mass accumulated upon the evaporator surface is related to the absolute humidity difference between evaporator air flow inlet and outlet, can be determined from

$$\dot{m}_{fr}=\dot{m}_a\,(\omega_{in}-\omega_{out}) \qquad (29)$$

Where the mass flow rate of air over the evaporator can be calculated as:

$$\dot{m}_a=\frac{\dot{m}_r(h_{r,out}-h_{r,in})}{h_{a,in}-h_{a,out}} \qquad (30)$$

The mass of frost accumulated on evaporator surface for each time step can be obtained by:

$$\Delta m_{fr}=\dot{m}_{fr}\times\Delta t \qquad (31)$$

A portion of water vapor transferred into the frost surface from moist air increases the frost layer density and the rest of it increases the frost thickness. For each time step, the change of frost thickness can be determined by:

$$\Delta\delta_{fr}=\frac{\Delta m_{fr}}{A_T\cdot\rho_{fr\_previous}} \qquad (32)$$

These values are added to the frost mass and thickness values of previous time step in order to obtain the values for current time step. The calculation is repeated for 6 hour.

$$m_{fr}=m_{fr\_previous}+\Delta m_{fr} \qquad (33)$$
$$\delta_{fr}=\delta_{fr\text{-}previous}+\Delta\delta_{fr} \qquad (34)$$

G. Correlations Used

1. Frost Density

The frost density is evaluated using empirical correlations of Tao et al as [16] :

$$\rho_{fst}=5.55.10^{-6}\left(\frac{d_o}{L}\right)^{-.137}.\omega_\infty^{-0.413}.T_i^{-0.997}.Re_d^{0.715}.Fo_d^{0.252}.\rho_{ice} \qquad (35)$$

Where the parameter T_i is the temperature difference between the water triple point and coil surface:

$$T_i=T_{triple}-T_S \qquad (36)$$

Each new step for calculation of frost thickness and heat transfer values require the surface temperature (Ts) to calculate value, which can be estimated from energy balance relation on the frost surface:

$$Q=Q_{sensible}+Q_{latent}=h_a\eta_s A_T(T_S-T_a)+m_{fr}h_{sg} \qquad (37)$$

2. Frost Thermal Conductivity

in this study the correlations by Seker et al [17] is used to determine the thermal conductivity of the frost;

$$K_{fr}=1.202.10^{-3}.\rho_{fst}^{0.963} \qquad (38)$$

H. Coefficient of Performance

The performance of refrigerators is expressed in terms of the coefficient of performance (COP), defined as:

$$C.O.P=\frac{\text{Refregrating effect}}{\text{Compressor work}}=\frac{h_1-h_4}{h_2-h_1} \qquad (39)$$

Where, the enthalpy for each point is illustrated in figure (6) for typical case. In order to calculate the degrees of superheating and sub-cooling, the following two equations were used:

$$T_{sup}=T_{evap,out}-T_{sat,evap} \qquad (40)$$
$$T_{sub}=T_{sat,cond}-T_{cond,out} \qquad (41)$$

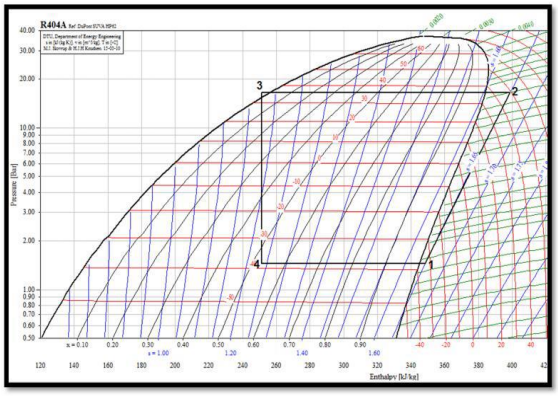

Fig. (6) Real test cycle in P-h Diagram for operating conditions as follows:

(T_{stor}=28.7ºC,RH_{stor}=25.6%,$T_{a,in}$=−14.41ºC,$T_{r,in}$=−36ºC).

I. Finding correlations of length and quality in the saturated portion of the evaporator

The quality of the refrigerant can be defined as;

$$x=\frac{m_g}{m_f+m_g} \qquad (42)$$

To solve these equations avoid fraction (α) equation needed to be added. This study adopted the modified X_{tt} model for void fraction equation. The modified X_{tt} model was selected from.

$$\alpha=(1+X_{tt}^{0.08})^{-0.378} \qquad X_{tt}\le 10 \qquad (43)$$
$$\alpha=0.823-0.157\ln X_{tt} \qquad X_{tt}>10 \qquad (44)$$

Where;

$$X_{tt}=\left(\frac{1-x}{x}\right)^{0.9}.\left(\frac{m_f}{m_g}\right)^{0.1}.\left(\frac{\rho_g}{\rho_f}\right)^{0.5} \qquad (45)$$

Also, the void fraction can be defined as : $\alpha=\frac{A_g}{A_C}$ (46)

If it is fatherly assumed that void fraction e is constant independent of L_{tp}, equation (41) can be written as follows:

$$x = \frac{\rho_g . A_C}{m_T} \int_0^{L_{tp}} \alpha . dL \quad (47)$$

J. Finding a correlation of heat transfer coefficient and quality in the saturated portion of evaporator

The rate of heat transfer for two-phase region can be determined from the following equation:

$$Q_{tp} = \dot{m}_r (x_{r,out} - x_{r,in}) h_{fg} \quad (48)$$

Also,

$$h_{r,tp} = \frac{Q_{tp}}{A_{tp}(T_{a,o} - T_{r,i})} \quad (49)$$

v. RESULTS AND DISCUSSION

A. Frost thickness and Frost mass accumulation for various operating conditions

Figures (7) and (8) shows that frost thickness and frost mass accumulation for three data sets (case1,case2 and case3) as shown in table (2),which increase with time as well as with relative humidity of air. The reasons for this increment due to relative humidity value depends on the amount of water vapor, any increase in this amount leads to increase in relative humidity, thereby increasing the thickness of the frost and mass accumulation.

Table (2) The operating conditions.

Data set	*RH%*	$T_{a,in}$℃	$T_{r,in}$℃	$\dot{m}_r$*(kg/s)*
Case1	30	-11.6	-38.08	0.01265
Case2	25	-11.9	-36.01	0.01272
Case3	20	-18.41	-38.81	0.01271

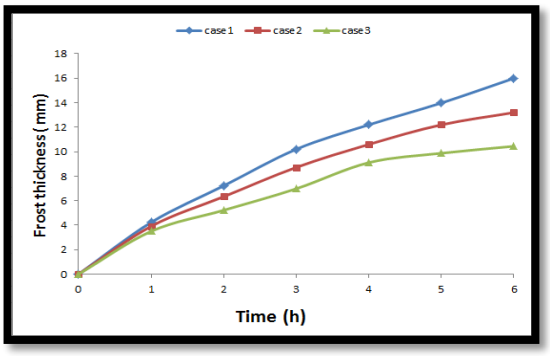

Fig.(7)Time-wise frost thickness variations.

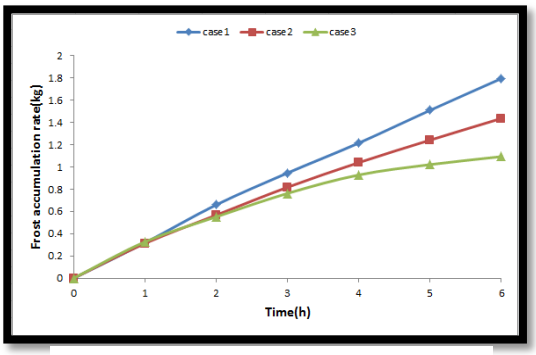

Fig.(8) Time-wise frost accumulation rate.

B. Air side pressure drop for different inlet relative humidity

The pressure drop characteristics show

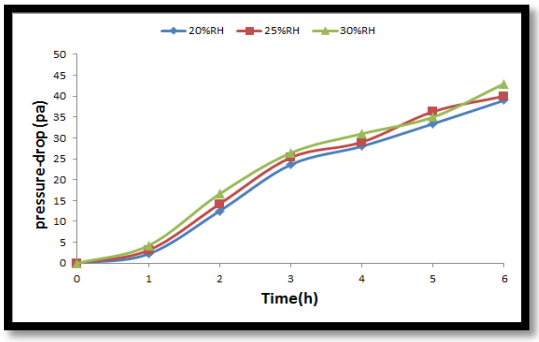

Fig. (9) Pressure drop characteristics.

exponentially increasing trend to relative humidity, as shown in figure (9). At the end of six hours the pressure drop increases almost

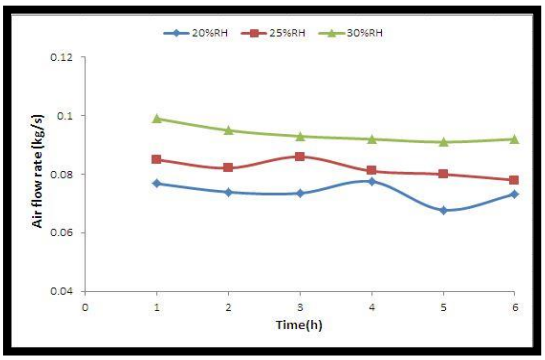

Fig. (10) Air flow rate change.

1.5 for the case of inlet relative humidity value of (30%RH) more than (25%RH) and twice more than (20%RH). The increase on pressure drop results in a decrease on airflow rate as shown in figure (10).

C. Overall heat transfer coefficient under frost growth conditions

Figure (11) shows the effect of relative humidity on total heat transfer coefficient for two-phase and superheated region respectively. The curves show decrease with time .This phenomenon can be explained as: One part of the water vapor flux on humid air condenses and solidifies on a frost surface and, consequently, increases the frost layer thickness. The other part of the water vapor flux penetrates by diffusion into the frost layer and increases frost density.

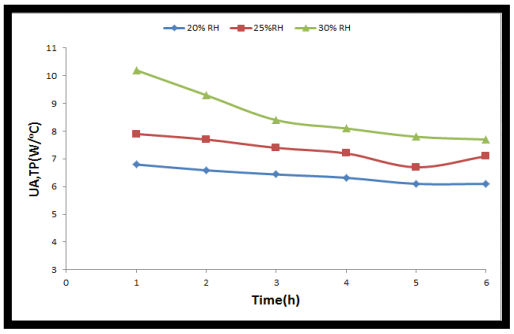

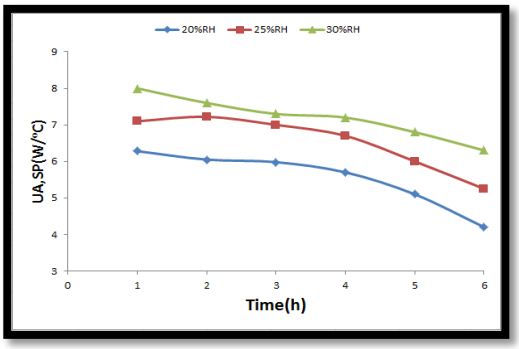

Fig. (11) Time-wise variations of the overall heat transfer coefficient of two-phase and superheated region, receptively.

D. Performance of the evaporator under frosting conditions

Simulation is carried out for six hours under frost formation with a store temperature of 28.7℃ and relative humidity RH=30%. As pressure drop increases, the air flow is dramatically decreased. After six hours, when the air flow rate decreases, the overall heat transfer coefficient between the air and evaporator will decrease, which in turn decrease the heat transfer rate. The drop in the evaporating temperature will cause a lower coefficient of performance, as shown in figure (12) and increased power consumption as shown in Figure (13). At the end of six hours of operation, the power consumption is about 9%than that of the first hour for typical case, this increase due to the increase in the frost thickness which represents as a thermal insulator on the surface of the evaporator.

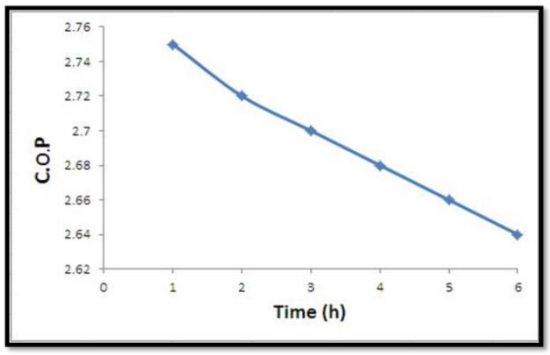

Fig. (12) Effect of frost on C.O.P.

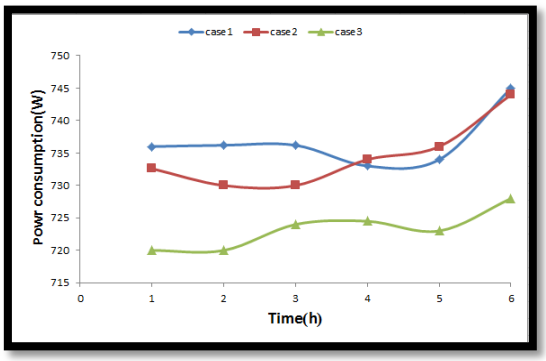

Fig.(13) Effect of frost on energy consumption for three cases of operating conditions.

E. Effect of superheating degree under frosting condition

The degree of superheated refrigerant at exit reduces from (3.6℃) to (1.6℃) at typical caseof operating ondition($T_{stor} = 28.7℃, RH_{stor}\% = 25.6, T_{a,in} = -14.41℃$, $T_{r,in} = -36℃, \dot{m}_r = 0.0125 kg/s$),due to less refrigerant boils off in the initial two-phase region .This, in turn will reduce the superheated length of the coil ,as shown in figure (14) .

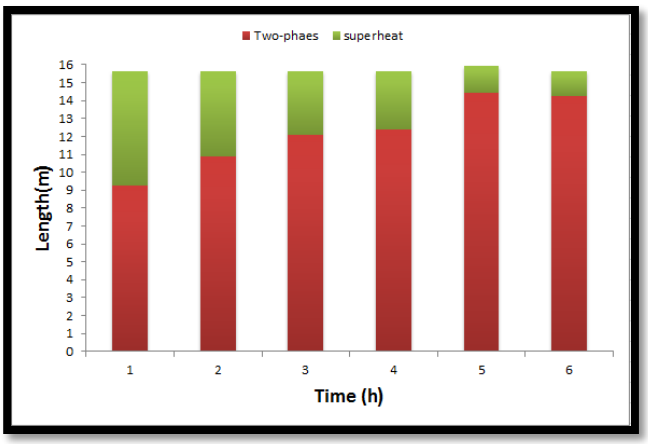

Fig. (14) Effect of frost on superheated length of evaporator

F. The correlations of length and heat transfer coefficient with quality in two-phase region under frosting conditions

As shown in figure (15) the length of evaporator in two-phase region is increased as quality of refrigerant increase, and the following new correlation can be obtained: { x=0.5+0.035L}.Also, figure (15) indicates that 30% of the total length is used in the quality range (0.85-1).

The internal heat transfer coefficient on figure (16) is highest at low qualities and it maintains a stable value from 70% to 80% beyond which.

The heat transfer declines rapidly. The correlation between the refrigerant heat transfer coefficient and the quality can be expressed as following:

$\{h_r = 651.08e^{-0.579x}\}$.

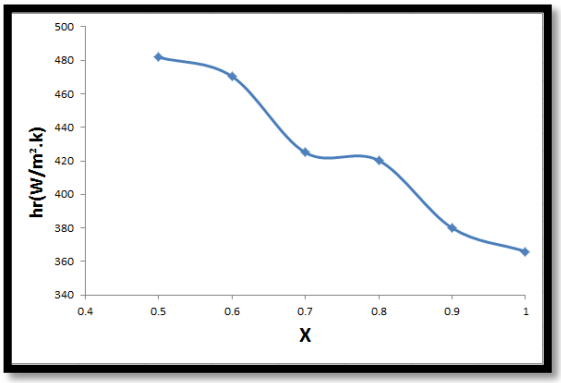

Fig.(14) Distribution of heat transfer coefficient with quality.

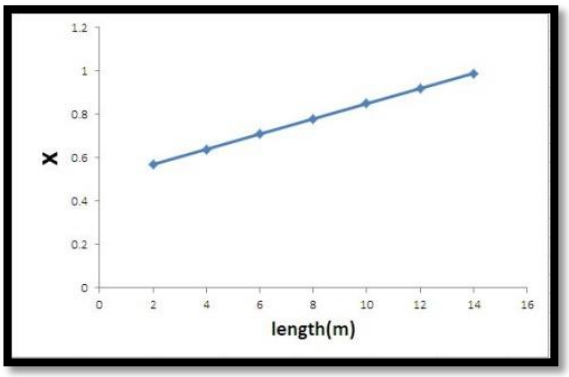

Fig. (15) Distribution of evaporator length with quality

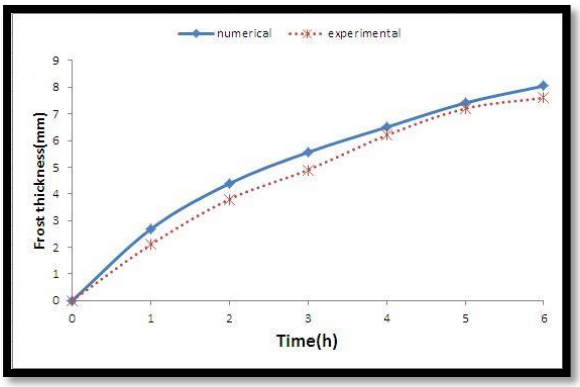

Fig. (16) Comparison of numerical and experimental frost thickness for five-row.

vi. MODEL VALIDATION

As shown in figure(16),the relative error of a numerically calculator frost thickness for evaporator five-row compared with experimental results is about 5%,depending on inlet parameters and the position for which the frost thickness has been compared. Also,the numerical results obtained have been validated against the experimental data taken by Geta and Bansal[12]employing different operating conditions .It was observed that the time-wise frost thickness distributions of present model have similar profile and behavior as in reference above.

vii. CONCLUSIONS

numerical model capable of being used as a design tool for display case evaporators was developed, validated and used. Important conclusions can be drawn from the present work. The effect of operating conditions on frost thickness and frost accumulation has been obtained. It can be concluded that the frost thickness and frost accumulation is faster when the inlet air humidity is higher. Frost growth significantly influences the heat transfer from air to refrigerant which evaporates inside the evaporator. During frost growth, both frost thickness and mass are found to increase simultaneously with time. Also the pressure-drop and frost thickness increased more rapidly for higher relative humidity values. The overall heat transfer coefficients$(UA)_{fr}$ under frosting conditions were calculated for two region in evaporator (two-phase and superheated), the increase in $(UA)_{fr}$ was about 1.3W/°C and about 0.9 W/°C for every 5% increase in the average store relative humidity for two-phase and superheated regions, respectively. At the stated operating condition, the values of $(UA)_{fr}$ were decrease with time for both regions(two-phase and superheated) due to frost formation. The simulation model was capable of predicting the power consumption which increases with time for different cases of operating conditions. In general, the model would be useful to the design engineers to evaluate the performance of display case evaporator under different operating conditions.

REFERENCES

[1] Deniz Seker,Hakan Karatas and Nilufer Egrican, (2004) " Frost formation on fin-and-tube heat exchangers Part I-Modeling of frost formation on fin-and-tube heat exchangers", International Journal of Refrigeration .27, 367–374.

[2] D.Datta, S.A.Tassou and D.Marriott, (1998)" Experimental Investigations into Frost Formation on Display Cabinet Evaporators in Order to Implement Defrost on Demand", Department of Mechanical Engineering, Brunel university, International Refrigeration and Air Conditioning Conference.

[3] C.P. Tso, Y.C. Cheng and A.C.K. Lai,(2006) "Dynamic behavior of a direct expansion evaporator under frosting condition. Part I. Distributed model", Science Direct, International Journal of Refrigeration 29, 611–623.

[4] H.M. Getu and P.K. Bansal, (2007)"Modeling and performance analyses of evaporators in frozen-food supermarket display cabinets at low temperatures", Science Direct, International Journal of Refrigeration 30, 1227-243.

[5] A.L.Bendaoud ,M.ouzzane,Z.Aidoun and N.Galanis, (2011)"Anovel Approach to study the performance of finned –Tube heat exchangers under frosting conditions",Faculté de Genie,Dé partement de Génie Mécanique,université de sherbrooke, Journal of Applied Fluid Mechanics, Vol. 4, Special Issue, pp. 9-20.

[6] Christian J.L.Hermes,chermes, (2013)"A. dimensionless correlation for the frost density", Laboratory of thermodynamics and thermophysics, Department of Mechanical Engineering, Federal University of Paraná, 22nd International Congress of Mechanical Engineering.

[7] Brunon.Borges,Cláudio melo and Christian J.L.Hermes, (2014)" Prediction of Evaporator Frosting in Household Refrigerators Subjected to Periodic Door Opening," 15th International Refrigeration and Air Conditioning Conference at Purdue, July 14-17.

[8] Alephzero (2014) ,www.alephzero.co.uk/ref/circeff.htm.

[9] EES,"A powerful tool for solving engineering problems and solving thermodynamic and heat transfer ",by VenkateshShanmugam,pro fessional V8.588-3D.
[10] F.P.Incropera,D.P.DeWitt, (2002)" Fundamental of Heat and mass transfer", John Wiley and Sons Inc ,pp.491-492.
[11] Hwang Y., Kim B.H. and Radermacher, (1997)" IIR international Transfer Issues in Natural Refrigeration".
[12] Incropera F.P. and D.P. DeWitt, (2002)"Fundamentals heat and mass transfer",John Wiley and Sons. 5th
[13] Ismail K.A.R. ,Salinas C.S.(1999) "Modeling of Frost Formation Over Parallel Cold Plates" Int. J. of Refrigeration, Vol.22, No 5, pp 442.
[14] Karatas H., (1996) "Theoretical and Experimental Investigation of a Domestic Refrigerator Evaporator", M.S Thesis,Istanbul Technical University.
[15] Kays WM and London AL, (1992)"Compact heat exchangers , 3rd ed.Singapore", McGraw Hill.
[16] Tao Y.X., Besant R.W, Rezkallah K.S. , (1993) "A Mathematical Model for Predicting the Densification and Growth of Frost on a Flat Plate", Int. J. Heat Mass Transfer, Vol. 36, No. 2, pp. 353-363.
[17] Seker.D ,H.Karatas and N.Egrican, (2004)"Frost formation on fin-and-tube heat exchangers.Part I:Modeling of frost formation on fin-and-tube heat exchangers."Int J Refrigeration27:367-74.

APPENDIX (A)

Expression to calculate the parameters Ω, S and F of equations (13) and (14)

$$\Omega = 0.00122\left(\frac{k_l^{0.79}.Cp_l^{0.5}.\rho_l^{0.49}}{\sigma^{0.6}\mu_l^{0.29}h_{lv}^{0.24}\rho_v^{0.24}}\right) \quad \text{(A.1)}$$

$$S = \frac{1-EXP\left(-F.h_l X_0/k_l\right)}{F.h_l X_0/k_l} \quad \text{(A.2)}$$

$$X_0 = 0.05\left[\frac{\sigma}{g\left(\rho_l-\rho_v\right)}\right]^{0.5} \quad \text{(A.3)}$$

$$F = \begin{cases} 1.0 & if \;\; X_{tt} \geq 10 \\ 2.0\left(0.213+X_{tt}^{-1}\right)^{0.736} & if \;\; X_{tt} < 10 \end{cases} \quad \text{(A.4)}$$

$$X_{tt} = \left(\frac{1-x}{x}\right)^{0.9}\left(\frac{\rho_v}{\rho_l}\right)^{0.5}\left(\frac{\mu_l}{\mu_v}\right)^{0.1} \quad \text{(A.5)}$$